Sensitivity of the Eddy Momentum Flux to Meridional Resolution in Atmospheric GCMs

ISAAC M. HELD AND PETER J. PHILLIPPS

Geophysical Fluid Dynamics Laboratory/NOAA, Princeton University, Princeton, New Jersey

(Manuscript received 31 May 1991, in final form 3 July 1992)

ABSTRACT

GCM experiments with zonally symmetric climates are used to demonstrate that the increase in the meridional eddy momentum fluxes and zonal surface winds that occurs when resolution is increased is primarily due to the increase in meridional rather than zonal resolution. It is argued that the sensitivity to meridional resolution reflects the need to resolve the small scales generated in the Rossby wave field as waves radiate from the midlatitude baroclinic eddy source region into regions with small mean winds. Some additional experiments highlight the sensitivity of surface winds and eddy momentum fluxes to the subgrid-scale horizontal mixing formulation in low-resolution models.

1. Introduction

A substantial amount of climate modeling research has been conducted with low-resolution spectral GCMs, typically using rhomboidal-15 (R15) or triangular-21 (T21) truncation. Among the problems that such low-resolution models possess, one of the most serious is that they underestimate the horizontal eddy momentum flux. This flux is found to increase very substantially when the resolution of the model is increased. The surface zonal winds also increase in strength since a larger surface stress is needed to balance the larger momentum flux convergence in the atmosphere. The large momentum flux in higher-resolution models has led modelers to include an estimate of the mountain torque due to subgrid-scale topography ("gravity wave drag") so as to avoid overestimating the strength of the Northern Hemisphere surface westerlies (Palmer et al. 1986).

This tendency of spectral atmospheric models with increasing resolution was documented by Manabe et al. (1978). Boer and Lazare (1988) describe broadly similar results. The systematic errors in the prediction model of the European Centre for Medium-Range Weather Forecasts, described by Tibaldi et al. (1990), paint the same picture: these systematic errors change relatively little once the resolution rises above T42, but the differences between the T21 and T42 models are large and qualitatively similar to that seen in other spectral models. Eliassen and Laursen (1990) describe similar results from a two-level model, and also point out that the momentum fluxes in their model are sensitive to the horizontal diffusivity. Boville (1991) has more recently described calculations in which the momentum fluxes continue to increase as the resolution is increased beyond T42.

The poleward heat flux by large-scale eddies is less sensitive to resolution than is the momentum flux. This is partly a consequence of the fact that if a climate model predicts too small a value for the atmospheric poleward eddy heat flux, self-correcting feedback comes into play: the meridional temperature gradient increases, enhancing the baroclinic instability of the flow and the associated heat flux. In addition, the static stability decreases if vertical eddy heat fluxes are weakened, further enhancing the instability. In contrast, if the horizontal eddy momentum flux in midlatitudes is underpredicted, the incentive for the model to correct this flux is relatively weak.

The *potential* for feedback does exist for the momentum fluxes. In particular, James and Gray (1986) have demonstrated that the momentum fluxes can feed back on the instability through the strength of the surface winds. The stronger the surface winds, the stronger the meridional shear in the zonal flow throughout the troposphere (think here of the meridional temperature gradients as being fixed), and this meridional shear tends to stabilize the flow to baroclinic instability. But the experiments outlined above clearly indicate that this "barotropic governor" is relatively weak compared to other feedbacks in the system, at least when the momentum flux is smaller than or comparable to the observed flux. It is likely that this feedback plays a more significant role when the system tries to create momentum fluxes that are *larger* than the observed flux.

A plausible explanation for the sensitivity of the momentum fluxes to model resolution follows from the relation between the momentum flux and merid-

Corresponding author address: Dr. Isaac M. Held, Geophysical Fluid Dynamics Laboratory/NOAA, Princeton University, P.O. Box 308, Princeton, NJ 08542.

ional wave propagation (e.g., Edmon et al. 1980). Baroclinic instability can be thought of as stirring the atmosphere in midlatitudes on certain space and time scales, exciting Rossby waves that propagate out of this strongly unstable region. The waves with the largest horizontal scales propagate into the stratosphere, while shorter waves are trapped within the troposphere and propagate meridionally, both polewards and equatorwards. Rossby waves propagating from their midlatitude region of excitation into the tropics produce the poleward eddy momentum flux in the subtropics. Although certainly oversimplified, it can still be qualitatively useful to think of these waves as linear, as propagating on a time-independent, zonally symmetric flow, and as approximately satisfying a local Rossby dispersion relation, in which $u - c$ is inversely proportional to the square of the total horizontal wavenumber $K^2 = k^2 + l^2$.

As a wave propagates meridionally away from the region of strong upper-level westerlies in midlatitudes and into regions of weaker westerlies, the zonal wavenumber and angular phase speed of the wave remain unchanged, but its meridional scale shrinks so as to continue to satisfy the local dispersion relation. Eventually the wave breaks, thereby mixing the fluid and decelerating the zonal flow. For detailed discussion of a particular example, see Held and Phillipps (1988). A model that does not possess sufficiently small scales to allow the waves to reduce their meridional scale appropriately will distort this meridional propagation and the associated momentum fluxes. In addition, a model that has insufficient horizontal subgrid-scale mixing, given its meridional resolution, will distort the wave-breaking process and the associated momentum flux deposition.

Shepherd's (1987) analysis of the enstrophy cascade in the atmosphere supports this emphasis on spectral evolution due to meridional propagation, as it shows that much of this cascade is, in fact, associated with wave–mean flow interaction and not with "fully developed" two-dimensional turbulence.

This picture suggests that it is the meridional, rather than zonal, resolution that is important for the simulation of the eddy momentum flux. To test this hypothesis, we compare the climates produced by GCMs with R15 and R30 resolution with a model that has the zonal resolution of the former and the meridional resolution of the latter. We use the notation Rm/n for a model that retains m zonal wavenumbers and n meridional modes for each of these zonal components. Therefore, we refer to this model as R15/30. For completeness, we also consider an R30/15 model, with the zonal resolution of R30 and the meridional resolution of R15. We also describe two additional R15 experiments, in which the strength of the subgrid-scale mixing is varied, that further illustrate the importance of the cascade to small scales for the surface wind and eddy momentum flux. We conclude with a discussion of the niche that the R15/30 GCM, or similar models, might be able to fill in the hierarchy of climate models.

2. The GCM

The GCM used in this work is identical to that used extensively for climate simulations by Manabe and collaborators at GFDL, except that the lower boundary condition has been simplified to be a flat, water-saturated, zero heat capacity surface with an albedo of 0.1. The drag coefficient used in the computation of the surface fluxes has been set equal to 1.0×10^{-3}, typical of oceanic values. Annual mean insolation is imposed at the top of the model, so that the model's climate is symmetric about the equator, as well as zonally symmetric. Clouds are not predicted; instead, a zonally symmetric cloud distribution is prescribed. The integrations are averaged over 1400 days, after discarding an initial spinup period. This length of integration is more than adequate for isolating the large changes in the subtropical momentum fluxes and midlatitude surface westerlies that we emphasize in this paper. (Because of the cross-equatorial symmetry of the boundary conditions, the two hemispheres provide more or less independent realizations and, therefore, some indication of the sampling error.)

The subgrid-scale mixing in the R30, R15/30, and R30/15 models is treated as biharmonic diffusion (e.g., $\partial_t \zeta = -\nu \nabla^4 \zeta$) with $\nu = 10^{16}$ m^4 s^{-1}. In the R15 climate model studies at GFDL, this same value of ν has been used, even though it is recognized that the resulting model does not dissipate strongly enough to resolve a smooth enstrophy cascade and prevent a buildup of enstrophy near the spectral cutoff wavenumber. As one increases the damping so as to better resolve the cascade, the damping of the dominant baroclinic eddies becomes significant. The close association between eddy momentum fluxes and the meridional cascade to small scales suggests that the behavior of the system should be studied as one varies the strength of subgrid-scale mixing, as well as the meridional and zonal resolution [as is also suggested by the two-level results of Laursen and Eliassen (1989) and Eliassen and Laursen (1990)]. As a step in this direction, the results for the R15 model are presented with two different values of the biharmonic diffusivity: 10^{16} and 10^{17} m^4 s^{-1}. We also describe an additional R15 experiment in which the damping is more scale selective (∇^8).

3. Results

Figure 1a shows the vertically averaged eddy momentum flux,

$$M \equiv p_*^{-1} \int \overline{u'v'} dp \qquad (1)$$

obtained from the R15, R15/30, R30/15, and R30 models. Figure 1b is a plot of the differences between

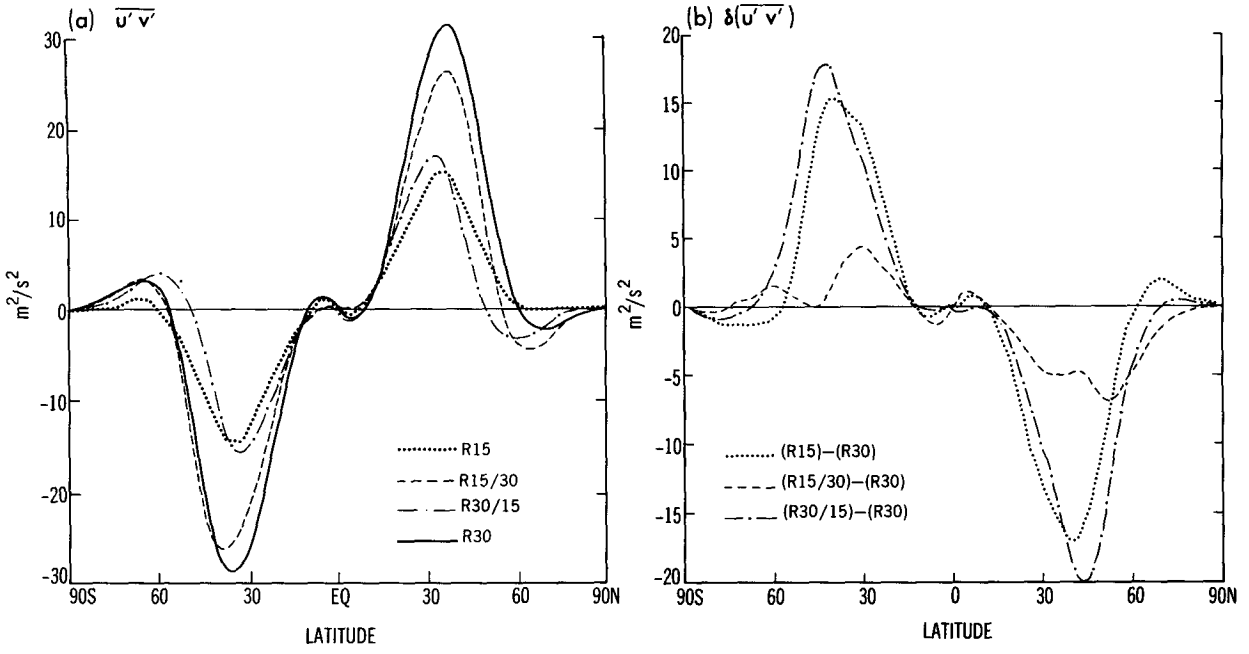

FIG. 1. (a) The vertically averaged eddy momentum flux in four GCM calculations with different resolutions. (b) The difference in the vertically averaged eddy momentum flux between R30 and the other three models.

the R30 result and the results from the other three models. Figure 2 is an analogous plot for the vertically averaged eddy flux of temperature

$$H \equiv p_*^{-1} \int \overline{T'v'}\,dp. \qquad (2)$$

As expected from previous work, the R30 model has twice as large a momentum flux as does the R15 model, while the midlatitude eddy heat flux is only slightly larger in R30 than in R15. The consistency between the hemispheres suggests that the small difference in heat flux is statistically significant. The R30 model also

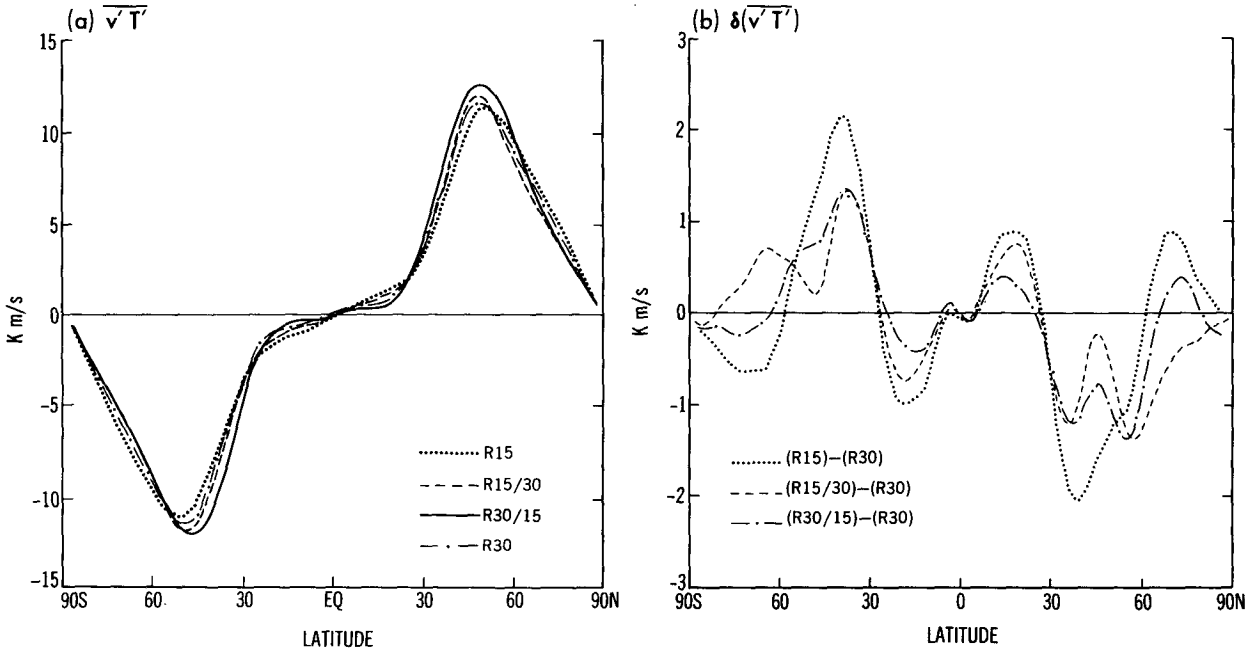

FIG. 2. As in Fig. 1 but for the vertically averaged eddy heat flux.

has less penetration of the eddy heat flux into the tropics and into the polar regions.

The R15/30 model generates momentum fluxes that are almost as large as those in R30, while the R30/15 model fluxes are much closer to R15, confirming that it is meridional, and not zonal, resolution that is the key difference between R15 and R30 in this regard.

For obscure reasons, R15/30 is the only model that does not possess a small, localized, equatorial momentum flux convergence, a signature of a tropical source of eddies. Also, R15/30 produces a heat flux that is intermediate in magnitude between R15 and R30. However, the penetration of the heat flux into the tropics evidently is more sensitive to zonal than meridional resolution, with the tropical eddy flux in R15/30 resembling R15 more than R30. Consistently, the eddy heat flux in R30/15 is somewhat closer to R30 in the tropics.

Figure 3 shows the zonal-mean zonal wind at the surface and at 205 mb, and the mean meridional wind at 205 mb, in these four models. We focus first on the R15 and R30 results. The midlatitude surface westerlies in R30 are nearly twice as strong as in R15, consistent with the momentum fluxes in Fig. 1, while the low-latitude easterlies are more than 50% stronger in R30. The polar surface easterlies are very much stronger, being hardly evident in R15. The equatorward eddy momentum flux at high latitudes in R30 is responsible for the strengthened polar easterlies.

At upper levels, the increase in the strength of the zonal winds in R30 is greater than the increase near the surface, so that the north–south temperature gradient has also increased (although there is still noticeable sampling error at upper levels, as indicated by the interhemispheric asymmetry). Since the midlatitude eddy heat flux in R30 is slightly *greater* than that in R15, this increase in temperature gradient must be attributed to the heat transported *equatorward* by the stronger Ferrel cell driven by the larger momentum fluxes. The balance

$$fv \approx -(a\cos^2(\theta))^{-1}\partial_\theta(\cos^2(\theta)\overline{u'v'}) \qquad (3)$$

is a very good approximation in the midlatitude upper troposphere. The stronger Ferrel cell is shown explicitly in Fig. 3c. Note also that the increase in the strength of the Hadley cell is even greater than that of the Ferrel cell.

Given the increase in the vertical shear evident in Fig. 3, it is surprising that the eddy heat flux does not increase more than is shown in Fig. 3. Perhaps the increased horizontal shears are a significant stabilizing influence, through the barotropic governor.

Turning to the mixed resolution models, we see that R15/30, with its high meridional resolution, matches the strength of the surface midlatitude westerlies in R30 and the strength of the Ferrel cell. In the tropics, R15/30 captures 2/3 to 3/4 of the increase in the easterlies that one achieves by increasing both zonal and merid-

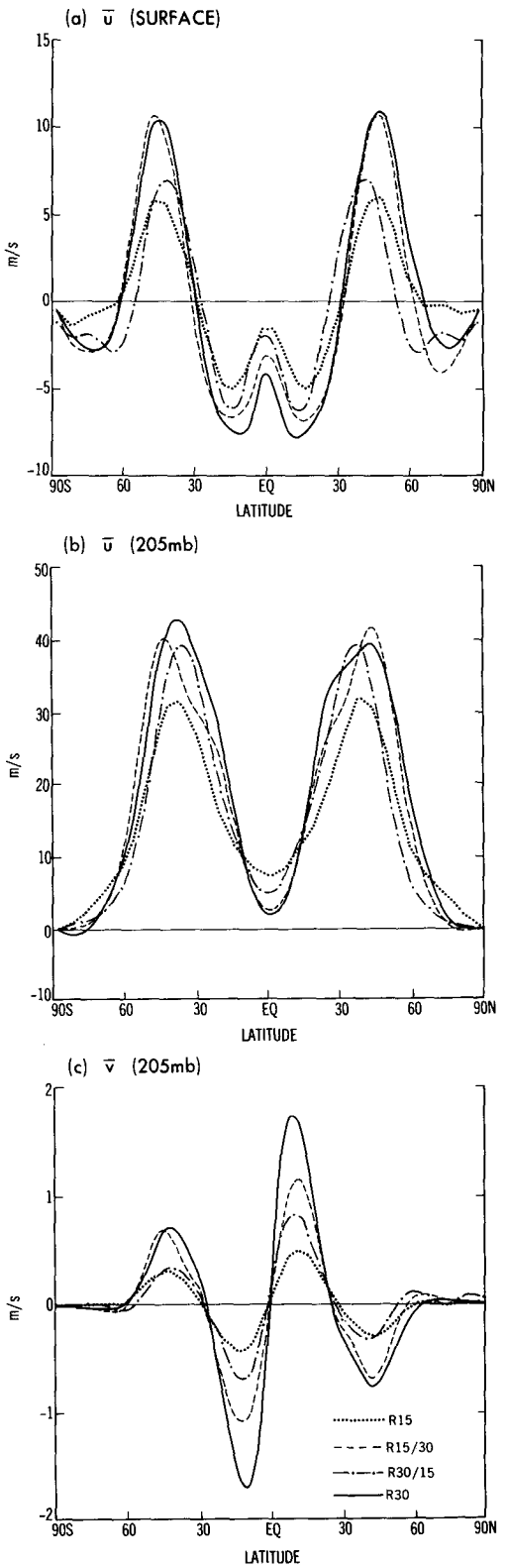

FIG. 3. The zonally averaged zonal wind (a) at the lowest model level and (b) at 205 mb, as well as the zonally averaged meridional wind at 205 mb (c), with the four truncations.

ional resolution. It also captures ½ to ⅔ of the increase in the strength of the Hadley cell at this level.

In contrast, the R30/15 model predicts surface midlatitude westerlies and a Ferrel cell of approximately the same strength as does R15. In the tropics, the easterlies are somewhat stronger than in R15, but still weaker than R15/30. The same relations hold for the strength of the Hadley cell in Fig. 4c. It appears that the effects of increasing zonal and meridional resolution on the strength of the Hadley cell and the trade winds are roughly additive, with the increase in meridional resolution provided roughly ⅔ and the zonal resolution ⅓ of the increase from R15 to R30.

Why the mean tropical flow should be sensitive to zonal resolution is unclear. We have confirmed, however, that the differences between the eddy momentum fluxes in the various experiments, although appearing to be small in Fig. 1, account for most of the difference in the low-latitude meridional flow. One must replace f by the absolute vorticity $f+\zeta$ to obtain an accurate balance of the form (3) in low latitudes, but the fractional change in the absolute vorticity between the various experiments is found to be small compared to the fractional change in v. Therefore, the difference between the models' meridional flows can still be explained from the differences in the eddy momentum fluxes.

In high latitudes, while the sampling error is substantial, it is clear that R15/30 and R30/15 are both more similar to R30, with its stronger low-level polar easterlies, than to R15. The surface wind distribution in R30/15 is displaced equatorward compared to the other models, as is most clearly seen by focusing on the boundaries of the surface westerlies. Why this should be the case is unclear to us.

The upper-level zonal winds in Fig. 3b are also somewhat puzzling. Both R15/30 and R30/15 show jet strengths that are comparable to R30. We have argued that the increase in the jet in R30 over R15 can be related, in part, to an increased temperature gradient due to a stronger Ferrel cell. This explanation fits with the result from R15/30, which has a Ferrel cell comparable in strength to that of R30, but does not explain why the jet strength in R30/15 is greater than that in R15. We suspect that the latter is related to the equatorward shift of the jet maximum, since the same temperature gradient is balanced by stronger wind shears at lower latitudes. The response of the subtropical jet to changes in eddy fluxes need not be straightforward, as is illustrated by the idealized model of Held and Phillipps (1990). A convincing explanation for these responses in terms of the changes in eddy fluxes would require the quantitative modeling of the zonally symmetric responses of the GCM to changes in eddy fluxes, preferably using an axisymmetric version of the GCM—a calculation not attempted here.

Figure 4 shows the difference between precipitation (P) and evaporation (E) in these four experiments.

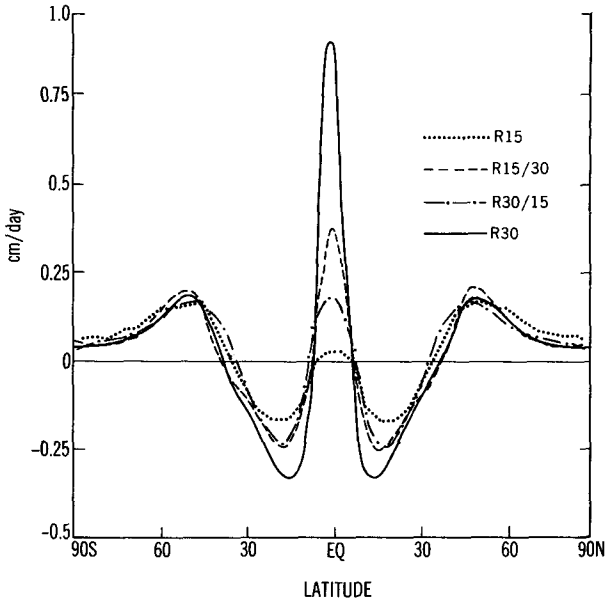

FIG. 4. Zonally averaged precipitation minus evaporation for the four truncations.

The equatorial values of $P-E$ are very sensitive to resolution, with R30 the largest and R15 the smallest. Not surprisingly, meridional resolution is more important than zonal resolution in sharpening and strengthening the intertropical convergence zone (ITCZ), although zonal resolution does contribute, consistent with its effect on the Hadley cell. The differences in high latitudes appear less pronounced, but in fact the values of $P-E$ for R30 are roughly a factor of two smaller than R15. Bottom water formation and the deep overturning oceanic circulation are sensitive to high-latitude sources of fresh water, so these differences would be very significant in coupled atmosphere–ocean models. Inspection of the moisture budget (not shown) indicates that most of this reduction in $P-E$ is due to the increased strength of the polar cell in R30, which transports moisture equatorward and out of polar latitudes, rather than to changes in the eddy moisture flux. Therefore, given the balance (3), it can be thought of as a direct consequence of the increased strength of the eddy momentum flux from high to midlatitudes. Much of this reduction in $P-E$ is also captured in the R15/30 and R30/15 models.

Figure 5a shows the difference in zonal mean temperature between the R15 and R30 models. Consistent with the change in vertical shear in Fig. 3, R15 has a smaller meridional temperature gradient, with polar temperatures in the midtroposphere $\approx$ 4 K warmer, and equatorial temperatures in the upper troposphere $\approx$ 4 K cooler, than in R30. (The "swamp" boundary condition is important for obtaining this substantial sensitivity of temperature to resolution; the sensitivity would presumably be smaller in models with realistic

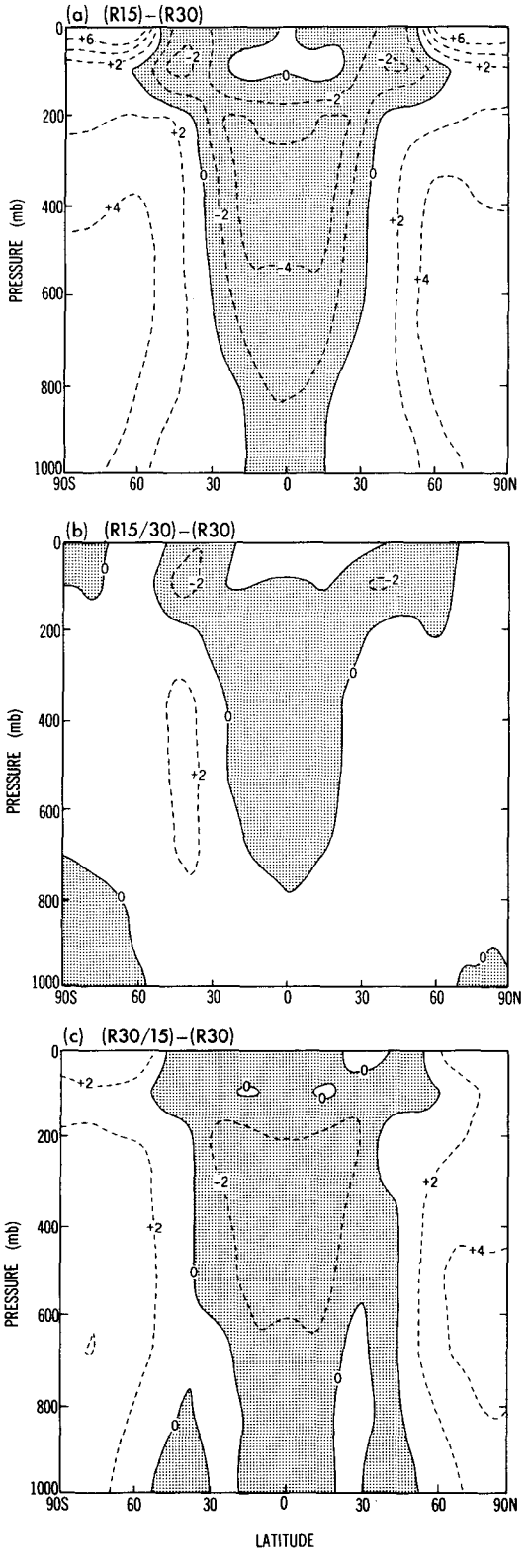

FIG. 5. (a) The difference in zonal mean temperature between the R15 and R30 integrations; (b) the analogous difference between R15/30 and R30; (c) between R30/15 and R30. The contour interval is 2 K, with negative values shaded.

boundary conditions and fixed ocean temperatures, but the energetically consistent "swamp" model is likely to be a better indicator of the sensitivity in a fully coupled model.) As discussed earlier, most of this difference can be attributed to the greater equatorward heat transport by the Ferrel cell in the R30 model. If we accept this picture, the transient eddies in high latitudes and the Hadley cell in low latitudes must then spread the news about the increased midlatitude gradient toward the pole and equator, respectively. This pattern is also probably affected by the larger penetration of the eddy heat flux into high latitudes in R15.

Figure 5b is the corresponding difference between the R15/30 and R30 models. This hybrid model is clearly in much better agreement with R30. It is slightly warmer than R30 in the subtropics and very slightly colder near the surface at the poles. For completeness, we also include the analogous plot for R30/15 in Fig. 5c, which is intermediate between R15 and R15/30.

4. Modified subgrid-scale mixing in the R15 model

While the preceding results point to meridional resolution as being the key to the large difference between the eddy momentum fluxes and surface wind distributions of the R15 and R30 models, the issue is complicated by the fact that the R15 climatology is sensitive to the subgrid-scale diffusion. Realizing that the R15 model with biharmonic diffusivity of 10^{16} m^4 s^{-1} is underdiffused, we have also examined a calculation with 10^{17} m^4 s^{-1}, as well as one with ∇^8 diffusion. In the latter case the diffusion coefficient is chosen so that the damping time for the largest meridional wavenumber at the zonal scale of the dominant eddies (which we take to be $m = 6$) is the same as the damping time for the largest meridional wavenumber, at the same zonal scale, in the R30 model with $\nu = 10^{16}$. (The resulting value is 8×10^{38} m^8 s^{-1}). In this way we imagine that during the quasi-linear meridional enstrophy cascade that occurs as a wave propagates into weaker zonal winds, diffusion will come into play with the same strength in the two models when the smallest permissible meridional scale is excited.

The surface winds produced in these two additional experiments are compared with the original R15 integration in Fig. 6a. The surface westerlies are increased in strength by $\approx$50% in both the enhanced ∇^4 and the ∇^8 cases, resulting in values that are only $\approx$2 m s^{-1} weaker than in the R30 model. It is also very clear that in both of these cases the high-latitude easterlies are much stronger than in the standard, low-diffusivity R15 integration.

The corresponding vertically integrated momentum fluxes are shown in Fig. 6b. The poleward fluxes in the subtropics remain much smaller than the R30 fluxes in both cases, having increased by only $\approx$20%. Closer inspection shows that the "improvement" in the surface westerlies is in part a consequence of the movement

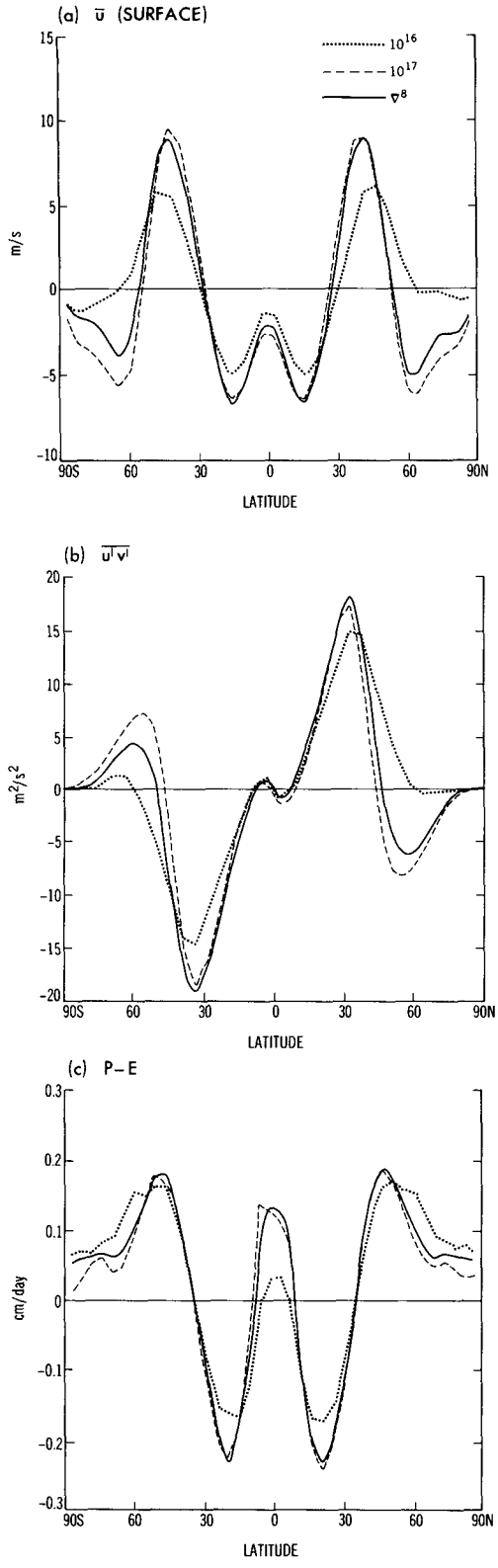

FIG. 6. Results for the R15 models with enhanced ∇^4 diffusion (10^{17}) and ∇^8 diffusion compared with the standard R15 integration: (a) zonal wind at lowest model level, (b) vertically integrated eddy momentum flux, and (c) precipitation minus evaporation.

of the subpolar zero crossing of the flux to lower latitudes, which enhances the flux convergence, and the larger equatorward fluxes at high latitudes. These R15 models exaggerate the polar easterlies, as compared with R30 (or R15/30), however. Our speculation is that stronger dissipation is preferentially damping some of the smaller-scale baroclinic instabilities at high latitudes in the R15 models, reducing the source of wave activity at high latitudes. This effect appears to be less severe in the ∇^8 calculation.

The stronger damping of small scales also has a beneficial effect on the hydrologic cycle, as evident in Fig. 6c. The ITCZ is better defined, because of the stronger Hadley cell driven by the larger momentum fluxes, although the value of $P - E$ at the equator is naturally still much weaker than that in the models with higher meridional resolution. The values of $P - E$ in high latitudes are also more similar to those in R30, due to the moisture transport out of the polar regions by the stronger direct meridional overturning. Therefore, when atmospheric models of this resolution are coupled to ocean models, we can anticipate significant sensitivity of the resulting ocean circulation to the atmospheric model's subgrid-scale diffusion, assuming that the ocean model is sensitive to the high-latitude values of $P - E$.

Finally, Fig. 7 shows the temperature difference between these R15 models and the R30 integration. With larger ∇^4 diffusion (Fig. 7b), the temperature field in the middle and upper troposphere is in better agreement with R30, but baroclinic instability has been suppressed (and the indirect Ferrel cell transport increased) to the point that the surface temperature difference between the subtropics and the poles is 3–4 K larger than in R30 (as opposed to 3–4 K *smaller* than R30 with the smaller value of the diffusivity). The more scale-selective ∇^8 model (Fig. 7a) seems to have a similar effect on the momentum fluxes as does the enhanced diffusion ∇^4 model, but without as strong a damping effect on the eddy heat transport.

5. Discussion

As computer power increases, many climate studies will be conducted with resolutions comparable to R30 or higher (in some cases, much higher). In spite of this tendency, relatively low-resolution atmospheric models, such as those discussed in this paper, will continue to play important roles in particular areas of research, most notably in studies of atmosphere–ocean interaction on ENSO time scales and, especially, on decadal-to-century time scales. A large number of lengthy integrations with a variety of models will be needed to understand this very low-frequency variability, and this is now feasible with low-resolution GCMs.

It has also become feasible to integrate these low-resolution models on workstations. This has the potential of dramatically increasing the number of sci-

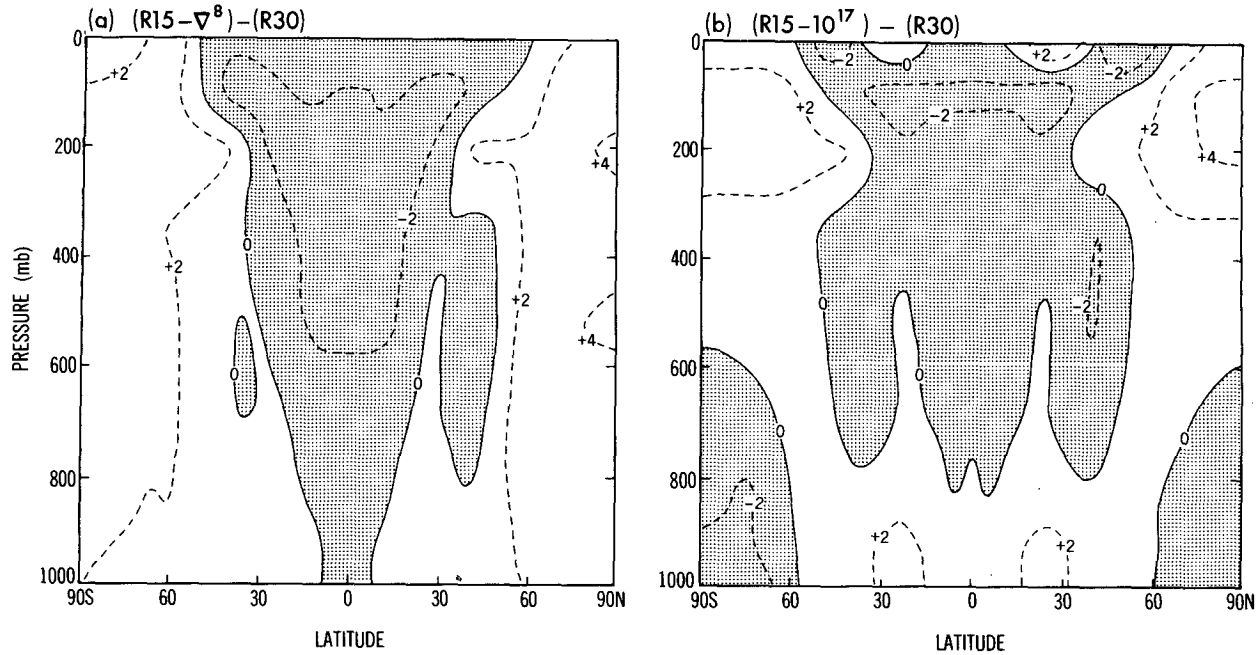

FIG. 7. As in Fig. 5 for the difference (a) between the R15 model with ∇^8 diffusion and R30, and (b) between the enhanced diffusion ∇^4 model and R30.

entists and students who have access to such models. Thus, although much of the work at the major modeling centers will naturally gravitate to higher-resolution studies, it remains important to try to improve the simulations in these relatively low-resolution spectral models.

In a GCM with a zonally symmetric climate, we find that the circulation produced by an R30 model can be fairly well approximated by a hybrid R15/30 model, with the meridional resolution of R30 and the zonal resolution of R15. This is particularly true for the strength of the eddy momentum fluxes, the surface westerlies, and the Ferrel cell. The deep tropical circulation retains some sensitivity to the zonal resolution. The climate of the R15 model is itself quite sensitive to the strength of the subgrid-scale damping, with the surface westerlies increasing in strength as the damping increases, and with the equatorward momentum flux in subpolar latitudes increasing in strength dramatically.

One could try to design a subgrid-scale damping scheme in the R15 model that minimized the difference between the R15 and R30 models, perhaps somewhat similar to the ∇^8 diffusivity described above, and then utilize this R15 model for long-term coupled model integrations. Given the importance of the meridional cascade to small scales for the atmosphere's momentum budget, and the absence of significant scale separation in the R15 model between the energy-containing eddies and the dissipation scale, we are more comfortable with the option of working with the hybrid R15/30 model.

In GCMs with explicit advection and implicit treatment of gravity waves, the time step is typically limited by *zonal* rather than meridional advection, due to the presence of strong zonal jets. In the integrations described above, the same time step was used for both the R15 and R15/30 models, while the R30 and R30/15 model integrations were performed with a step one-half this size. As a result, the R15/30 model was roughly a factor of two more time consuming than R15, and a factor of 4 more efficient than R30.

A model truncated in a manner similar to that of the R15/30 model seems to be a logical choice for ENSO studies, where adequate eddy momentum fluxes are essential for driving realistic trade winds, and where meridional resolution of the flow is of more concern than zonal resolution. It also appears to be a natural choice for coupled model studies of variability in the Southern Ocean, where the surface westerlies play a key role and where, once again, high zonal resolution in the atmosphere may not be essential.

Acknowledgments. We thank S. Manabe and A. Broccoli for helpful comments on an earlier draft of this manuscript, and the Scientific Illustration Group at GFDL for assistance with the figures.

REFERENCES

Boer, G. J., and M. Lazare, 1988: Some results concerning the effect of horizontal resolution and gravity-wave drag on simulated climate. *J. Climate,* **1,** 789–806.

Boville, B. A., 1991: Sensitivity of simulated climate to model resolution. *J. Climate,* **4,** 469–485.

Edmon, H. J., B. J. Hoskins, and M. E. McIntyre, 1980: Eliassen–Palm cross-sections for the troposphere. *J. Atmos. Sci.*, **37,** 2600–2616.

Eliassen, E., and L. Laursen, 1990: On the effects of horizontal resolution and diffusion in a two-layer general circulation model with a zonally symmetric forcing. *Tellus,* **42A,** 520–530.

Held, I. M., and P. J. Phillipps, 1987: Linear and nonlinear barotropic decay on the sphere. *J. Atmos. Sci.*, **44,** 200–207.

——, and ——, 1990: An idealized model of the interaction between the Hadley cell and a Rossby wave. *J. Atmos. Sci.*, **47,** 856–869.

James, I. N., and L. J. Gray, 1986: Concerning the effect of surface drag on the circulation of a baroclinic planetary atmosphere. *Quart. J. Roy. Meteor. Soc.*, **112,** 1231–1250.

Laursen, L., and E. Eliassen, 1989: On the effects of damping mechanisms on an atmospheric general circulation model. *Tellus,* **41A,** 385–400.

Manabe, S., D. G. Hahn, and J. L. Holloway, 1978: Climate simulations with GFDL spectral models of the atmosphere. Report of the JOC study conference on climate models: Performance, intercomparison, and sensitivity studies. GARP Publication Series No. 22, Vol. 1, WMO, Geneva, 41–94.

Palmer, T. N., G. J. Shutts, and R. Swinbank, 1986: Alleviation of systematic bias in general circulation and numerical weather prediction models through orographic gravity wave drag parameterization. *Quart. J. Roy. Meteor. Soc.*, **112,** 1001–1039.

Shepherd, T. G., 1987: A spectral view of nonlinear fluxes and stationary-transient interaction in the atmosphere. *J. Atmos. Sci.*, **44,** 1166–1177.

Tibaldi, S., T. N. Palmer, C. Brankovic, and U. Cubasch, 1990: Extended-range predictions with ECMWF models: Influence of horizontal resolution on systematic errors and forecast skill. *Quart. J. Roy. Meteor. Soc.*, **116,** 835–866.